

Three Dimensional Numerical Simulation of a Full Scale CANDU Reactor Moderator to Study Temperature Fluctuations

A. Sarchami, N. Ashgriz, M. Kwee

Abstract—Threedimensional numerical simulations are conducted on a full scale CANDU Moderator and Transient variations of the temperature and velocity distributions inside the tank are determined. The results show that the flow and temperature distributions inside the moderator tank are three dimensional and no symmetry plane can be identified. Competition between the upward moving buoyancy driven flows and the downward moving momentum driven flows, results in the formation of circulation zones. The moderator tank operates in the buoyancy driven mode and any small disturbances in the flow or temperature makes the system unstable and asymmetric. Different types of temperature fluctuations are noted inside the tank: (i) large amplitude are at the boundaries between the hot and cold (ii) low amplitude are in the core of the tank (iii) high frequency fluctuations are in the regions with high velocities and (iv) low frequency fluctuations are in the regions with lower velocities.

Keywords—Bruce, Fluctuations, Numerical, Temperature, Thermal hydraulics

I. INTRODUCTION

CANADIAN DEUTERIUM URANIUM (CANDU) nuclear reactor is a Pressurized Heavy Water Reactor (PHWR) using heavy water as moderator in a horizontal, cylindrical tank (the *calandria tank*) to bring the fast neutrons from the fission reaction to the thermal neutron energy levels. The CANDU power reactor is comprised of few hundred horizontal fuel channels in a large cylindrical calandria vessel. Each fuel channel consists of an internal pressure tube (containing the fuel and the hot pressurized heavy water as primary coolant), and an external calandria tube separated from the pressure tube by an insulating gas filled annulus. The calandria vessel contains cool low-pressure heavy-water moderator that surrounds each fuel channel.

There have been numerous experimental studies on the operation of CANDU reactors. Koroyannaski et al [1] experimentally examined the flow phenomena formed by inlet flows and internal heating of a fluid in a calandria cylindrical vessel of SPEL (Sheridan Park Engineering Laboratory) experimental facility. They observed three flow patterns inside test vessel and their occurrence was dependent on the flow rate and heat load.

A. Sarchamiis with the University of Toronto, 5 King's College Road, Toronto, M5S 3G8, Canada (phone: 647-686-4440; e-mail: sarchami@mie.utoronto.ca).

N. Ashgriz, is with the University of Toronto, 5 King's College Road, Toronto, M5S 3G8, Canada (phone: 647-686-4440; e-mail: ashgriz@mie.utoronto.ca).

M. Kweeis with the Bruce Power, Toronto, Canada (e-mail: marc.kwee@brucepower.com).

In addition, there have been several CFD models for predicting the thermal hydraulics of the CANDU moderator. Yoon et al. [2] used the CFX-4 code to develop a CFD model with a porous media approach for the core region, while Yu et al. [3] used the FLUENT code to model all the Calandria tubes as heating pipes without any approximation for the core region.

Khartabil et al. [4] conducted three-dimensional moderator circulation tests in the Moderator Test Facility (MTF) in Laboratories of Atomic Energy of Canada Limited (AECL). MTF is a ¼ scale of CANDU calandria. MTF is designed to study moderator circulation at scaled conditions that are representative of CANDU reactors. The real time data recording at various locations inside the MTF tank have shown some level of fluctuations in the moderator experimentally measured temperatures

The purpose of the present study is to determine the causes for and the nature of the moderator temperature fluctuations using three-dimensional simulation of full scale Bruce tank with volumetric heating.

II. PROBLEM SETUP

The Bruce tank comprises of 8458 mm diameter cylindrical tank with 5940 mm length, eight inlet nozzles, two pipes as outlets at the bottom of tank, and 480 tubes.

During the normal operation of CANDU reactor, the cold moderator water enters the tank through eight nozzles, four nozzles at each side, and heated fluid exits from two outlet pipes at the bottom of the tank. The operating conditions for Bruce used in the simulation is listed in Table 1.

TABLE I
BRUCE B OPERATING CONDITIONS

NOMINAL CONDITIONS	BRUCE B, 50% FP
Power (kW)	64500
Average heat source	277 KW/m ³
Moderator mass flow rate (kg/s)	948.0
Inlet temperature (°C)	44.8

Fluent software V.12 is used as the numerical code for the simulation. The simulation is performed using unsteady, 2nd order implicit solver. RNG k-epsilon model with wall functions are used for turbulence modeling. Buoyancy effects are accounted for in the fluid density calculation method and the energy equation is solved for heat transfer inside the tank. An unstructured non-uniform tetrahedral and hexahedral mesh was used to construct meshes in the full Bruce tank. A total of 3,200,000 meshes were generated using the commercial software Gambit.

III. RESULTS

A. Temperature and Velocity Distributions

Temperature and velocity contours are presented here. The hot zone changes by time and space as shown in Figure 1. Figure 2 shows temperature and velocity contours for a plane called S at two different times, $t=20s$ and $t=150s$. The hot zone is on the left hand side while the jet impingement zone is located on the right hand side of the plane. Although the hot zone retracts to a smaller area at the top left corner, but it is visible throughout the simulation. The buoyancy forces are strong here due to the high heat flux. As a result, the buoyancy forces prevail those of momentum and create a hot region at the top of the tank. The highest observed temperature is $730^{\circ}C$ at the core of the hot zone and $500^{\circ}C$ near the outer wall, far from the hot zone and near the jet impingement area.

The velocity contours show that the highest velocities are visible on the outer wall where the inlet nozzles are located. Although there are no inlet nozzles located at this specific plane, but their effects on the flow field is clearly visible.

The highest observed velocities are about 1.3 m/s near the wall and go below 0.2 m/s in the core of the tank far from the injection and impingement areas. The jet impingement point and the secondary jet penetration are traceable in the figure. The penetration depth of the secondary jet is relatively poor, reducing the level of mixing inside the tank. This will increase the segregation between the high temperature and the low temperature zones. Consequently, both temperature and velocity fluctuations can be higher at the boundaries between the high and the low temperature and velocity zones. The other implication of poor jet penetration into the tank is that it will have less cooling effect since the cold jets will pass through less number of tubes.

Figure 3 shows temperature distribution in plane D1, which is located in XZ plane. This plane provides a top view of the tank, showing how the temperature and velocities are distributed along the length of the tubes. A highly asymmetric flow is observed here. The hot region is located in the front section with temperatures as high as $700^{\circ}C$ and the colder regions are at the back side of the tank with temperatures as low as $480^{\circ}C$.

As time proceeds, hot region starts to shrink and at $t=150s$, almost the entire high temperature region (i.e. $730^{\circ}C$) existing at $t=20s$ is vanished. Although the high and low temperature regions are still distinguishable, but the distribution shows better mixing in comparison with previously presented planes. This can be the result of flow fields in XZ plane, which circulates the flow throughout the tank and results in a better homogeneity in temperature distribution. The velocity distribution shows that there are two high velocity regions at both side of the tank. The velocities at those regions are in the range of 1.3 m/s . The velocities in the hot regions are lower (below 0.2 m/s) than those in the colder regions (below 0.5 m/s), indicating relatively poor mixing in the hot regions. The buoyancy forces are dominant in those regions and momentum forces are unable to produce enough mixing to have lower and more even temperatures.

B. Temperature and Velocity Fluctuations

Temperature and velocity fluctuations with time are presented here. Total of 55 points with different coordinates are considered for monitoring and result analysis and only some of them will be presented in this paper. Figure 4 shows the temperature and velocity plots for various points inside the tank. Points 5, 6, and 8 are located at the center of the tank, $x=y=0$.

The mean temperature shows a very slow frequency oscillation, indicating that the hot fluid zone slowly moves back and forth. The amplitude of fluctuations for points around the center part of the tank, are small, since these points are inside the hot zone and away from the boundaries of the hot zone. Point 6 has a temperature of about $700^{\circ}C$ prior to $t=50s$, but it decreases to a temperature of less than $680^{\circ}C$ at the end of the simulation. Its velocity varies between 0.06 m/s and 0.14 m/s , which are considered as low velocities, with mean values of about 0.1 m/s . Flow through this point is mainly due to the bulk flow in the core of the tank, and therefore, it has small fluctuation amplitudes. Point 8 is inside the hot zone, but intermittently cold flow enters this zone, resulting in sharp drops in temperature. Velocity at this point is less than 0.07 m/s during the first 80 seconds. The fluctuations are low in amplitude and medium in frequency. The mean velocity remains around 0.065 m/s and no general increase or decrease is observed in velocity. Passing through $t=80s$, the nature of fluctuation changes, resembling point 6 with lower frequencies and noticeably higher amplitudes. The mean velocity increases to 0.1 m/s and stays at this value until the end of the simulation. This point is located on the same plane as injection nozzles. At the start of the simulation small amplitude-medium frequency fluctuations are observed. These are due to the cold inlet flows at high velocity interacting with the bulk fluid inside the tank. After certain time, the flow develops inside the tank and injection effects diminish at point 8 and the bulk fluid movements take effect. This is the time when the fluctuations become similar to point 6 since the driving force behind both are bulk fluid flow inside the tank.

Points 45, 49, and 50 are close to the high velocity wall jet flows and they have relatively high frequency fluctuation. The temperature at point 45 is relatively low, with a maximum temperature of $590^{\circ}C$. This point is located between the hot and the cold regions, near the jet penetration path. Therefore, it has a high frequency temperature fluctuation as the hot and cold fluid zones come in and out of it. Point 49 is located further to the left and closer to the outer wall with respect to point 45. The mean velocity is around 0.3 m/s throughout the simulation. Maximum velocity at some instances is close to 0.8 m/s and minimum velocity goes as low as 0.1 m/s .

Temperature and velocity fluctuations at point 50 have high frequency. The mean velocities are around 0.55 m/s and high amplitude since the point is close to the boundary between hot and cold. Point 50 has a mean temperature of $620^{\circ}C$ with maximum and minimum temperatures of $660^{\circ}C$ and $580^{\circ}C$, respectively. The temperature fluctuation in this point is high in both amplitude and frequency. At some intermittent times, its temperature varies by more than $60^{\circ}C$ in short time. The

maximum velocity for this point during the simulation is close to 0.9 m/s and the minimum velocity is less than 0.3 m/s. The mean velocity at this point remains almost constant throughout the simulation at around 0.6 m/s.

C. Main Flow Regimes

Simulation results show an asymmetry in temperature distribution in all three directions inside the tank. Figure 5 shows three planes in Z direction and one plane in Y direction. These planes essentially cover the entire tank and show the asymmetry in every direction. Generally, high temperature areas are concentrated close to the symmetry plane ($z=0$) and the upper parts of the tank. Ideally when the cold water penetrates from the impingement point at the top of the tank, the flow passes through a large number of tubes and exits the tank with high temperature. But instead, the hot zone lies at the top and the flow which passes through the tubes does not pass through many numbers of tubes. These two factors greatly reduce the cooling effects inside the tank.

Three different flow regimes can be identified inside the tank. These flows are:

- *Inlet jet impingement flows:* These are the flows generated due to the inlet nozzle flows which go through the upper edge of the tank, impinge on each other, and form downward moving flows.

- *Buoyancy-driven flows:* There is a strong flow at the left hand side, which passes through the tubes but goes toward the top of the tank. This is against the bulk flow regime and is mainly due to the strong buoyancy forces inside the tank

- *Clock-wise flow:* This flow is the strongest in symmetry plane and it occupies almost $\frac{3}{4}$ of periphery of the tank. It consists of two sub-flows. The first one comes from the right nozzle to the bottom of the tank and the second sub-flow runs from the left nozzle to the top of the tank.

The temperature plot shows that temperature increases from the inlet toward the impingement point. This is expected since as flow passes through the tubes and interacts with hot water inside the tank, its temperature increases more than 15°C for the left jet and less than 10°C for the right jet. The average temperature is also higher for the left jet compared with the right jet.

This is due to two main factors:

- The impingement point is on the right side of the tank and the left jet travels a longer distance to the impingement point. Therefore, it heats up more.

- The hot zone is pushed to the left and therefore, the left jet passes through a hot boundary, which causes an increase in its temperature compared with the right jet.

The velocity plot shows that the inlet jets lose their momentum as much as 90% by the time they reach to the impingement point. The velocity decreases from about 1 m/s at the nozzle inlet to less than 0.5 m/s at the impingement point. This is not desirable since low impingement velocities produce low-momentum secondary jet that cannot penetrate the tank efficiently. Consequently the cooling efficiency of the inlet jets reduces. The velocity of the secondary jet also decreases by distance from the impingement point. The

secondary jet only carries 10% of the initial momentum injected by the inlet nozzles. Half way through its path, the secondary jet has lost 80% of its already small initial momentum. This greatly reduces the mixing inside the tank and by the time the flow is near the exit, the inertia is not the driving force anymore and flow becomes buoyancy driven.

Temperature increases and velocity decreases as the secondary jet goes toward the outlet pipes. Near the outlet the flow stream has very low velocity and high temperature. Most of the hot flow which has lost most of its momentum turns around (creating circulation zone at the bottom) and moves toward the top of the tank at the left hand side instead of going to the outlet pipes. This contributes to the hot and cold zones segregation inside the tank.

IV. CONCLUSION

The fluid and thermal behavior inside the tank can be generally described as follows: The cold inlet flows through nozzles on the right and the left sides of the tank tend to move on the outer boundaries towards the top of the tank. These flows are referred to as the “*wall jet flows*”. The wall jet flows from the right and the left sides of the tank impinge on each other somewhere on the top of the tank. This results in a secondary downward moving jet which penetrates into the tube bundles. This jet is referred to as the “*secondary jet flow*”. The inlet jets lose 90% of their momentum upon reaching to the impingement point. The velocity of the secondary jet further reduces once it reaches bottom of the tank. It only carries 20% of its initial momentum. Generally, the secondary jet divides the tank into two sides. One side contains high temperature liquid and the other side contains low temperature liquid. The impingement point is not necessary at the top center of the tank and it is shifted towards one side. In 3D simulations, the impingement point is closer to the right side of the tank (with respect to the flow direction in the fuel channels). The numerical results show that the flow and temperature distributions inside the moderator tank are completely three dimensional and no symmetry plane can be identified. Temperature contours in different planes show the hot regions at the top and the left-hand side (close to the center line) of the tank. The temperature contours along the length of the tank have a saddle shape, with high temperatures towards the edges of the saddle. This is due to the strong wall jet flows in the middle planes pushing the hotter fluid towards the end walls of the tank. Competition between the buoyancy driven flows and the momentum driven flows may result in various flow distribution modes inside the tank. The competition between the downward moving momentum driven flows (induced by the secondary jet) and the upward moving buoyancy driven flows results in the formation of circulation zones inside the tank. One of the determining factors of the size of the circulation zones is the strength and penetration length of the secondary jet flow. The numerical results indicate that the moderator tank operates in the buoyancy driven mode, since the cold wall jet flows and the secondary jet flows remain mainly at the outer boundaries of the tank. Any small disturbances in the flow or temperature can make

the system unstable and asymmetric. Once the system comes out of symmetry, it cannot go back to symmetry. This in fact occurs in the moderator tank, resulting in circulating hot buoyancy driven flow at one side and a cold momentum driven flow at the other side of tank.

Any small disturbances in the flow, such as flow past tube bundles, are amplified by the buoyancy effects. In particular, the segregation of hot and cold flow zones, combined with flow fluctuations results in relatively large amplitude temperature fluctuations at the boundaries between the hot and cold zones. The following conditions are observed:

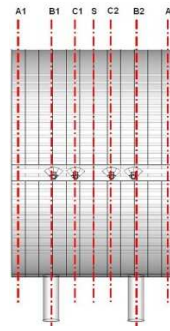
- Large amplitude temperature fluctuations are mainly at the boundaries between the hot and cold (e.g., outer boundaries of the bundle, regions close to the penetrating secondary jet flows).
- Low amplitude temperature fluctuations are mainly in the core of the tank with more uniform temperature distributions (e.g., central and lower parts of the tank).
- High frequency fluctuations are in the regions with high velocities (e.g., top boundaries at the interface between the wall jet flows and the inner core flows, regions close to the penetrating secondary jet flows).
- Low frequency fluctuations are in the regions with lower fluid velocities (e.g., inner core).

Therefore, there are categorized as high-frequency-high-amplitude, high-frequency-low-amplitude, low-frequency-high-amplitude, and low-frequency-low-amplitude.

Depending on the location of the monitored point the behavior of the fluctuations are different. Points which lay near the hot and cold boundaries have higher frequencies and depending on the conditions high or low amplitudes. Points located close to the core and far from the mixing zone have less chaotic behavior and the frequencies are lower. Very low frequencies with comparably high amplitudes can be attributed to the bulk fluid regimes inside the tank rather than local mixing phenomenon.

Velocity contours show relatively small velocities throughout the tank. The bulk fluid is moving with steady and slow pace and most of the momentum action is observed near the injection nozzles, penetration path, and boundaries between low and high velocity flows. Higher velocities are expected in the latter case since considerably higher mass flux is coming into the tank.

There is also a secondary flow formed by the impingement of the flows from the two neighboring inlet jets. Since the nozzles are designed to distribute the flow along the length of the tank, the flow from neighboring jets impinge on each other. This impingement flows creates a clock-wise circulating flow in the symmetry plane. This circulating flow is the strongest in the symmetry plane and the nozzle plane without exit pipe and it is the weakest in the nozzle plane with the exit pipe, which is mainly dominated by the bulk flow from the inlet nozzles to the outlet pipe. This clock wise circulating flows weaken the right inlet flows, contributing to the movement of the impingement point to the right hand side of the tank.



Space

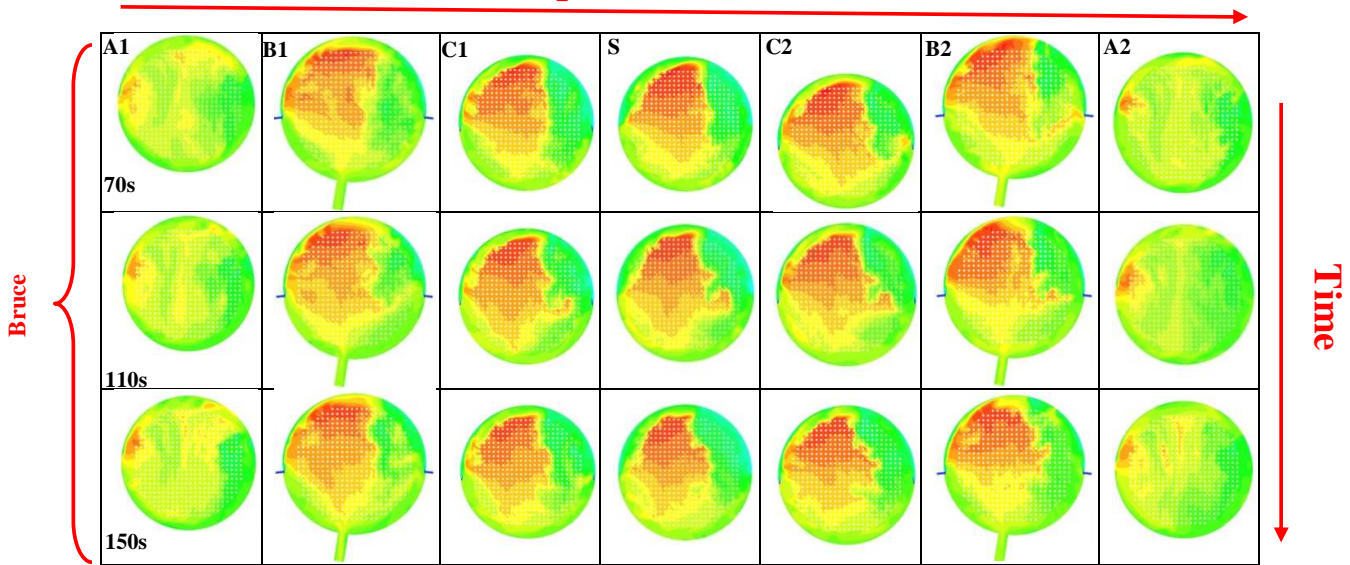


Fig. 1 Temperature distribution inside the tank in different planes in various times

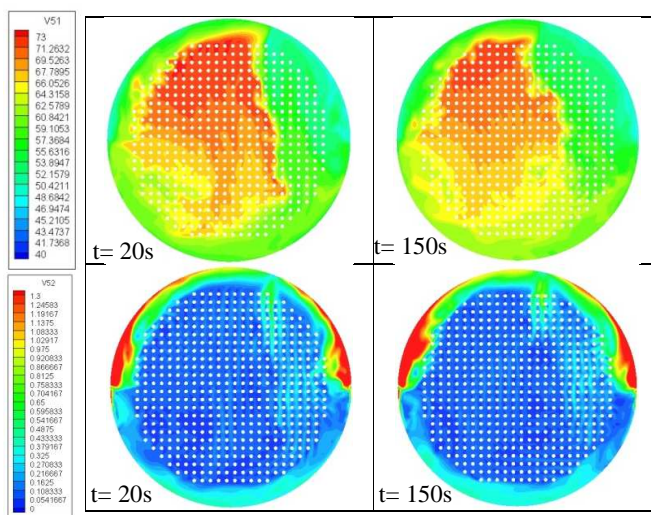


Fig. 2 Temperature and velocity contours in various times for plane S

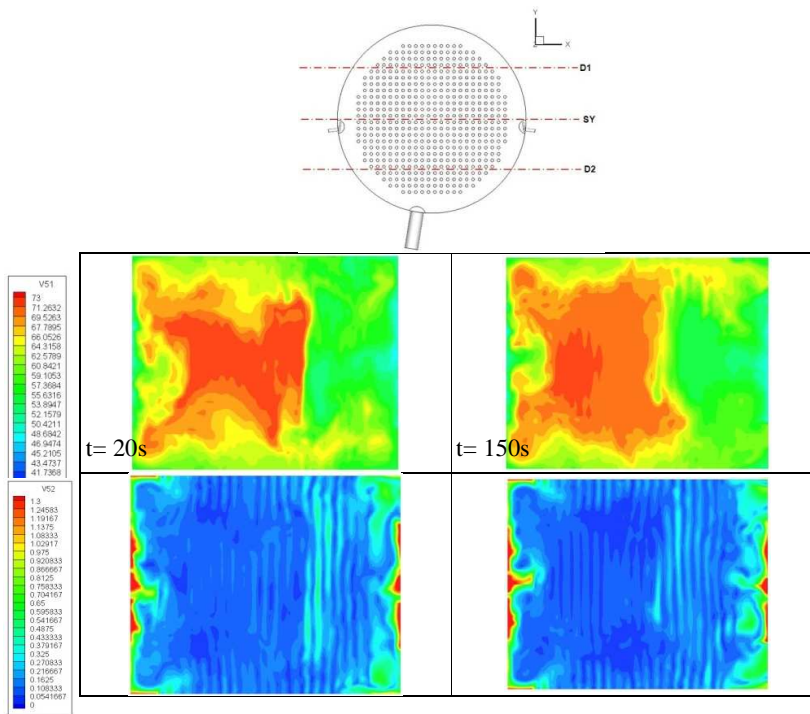


Fig. 3 Temperature and velocity contours in various times for plane D1

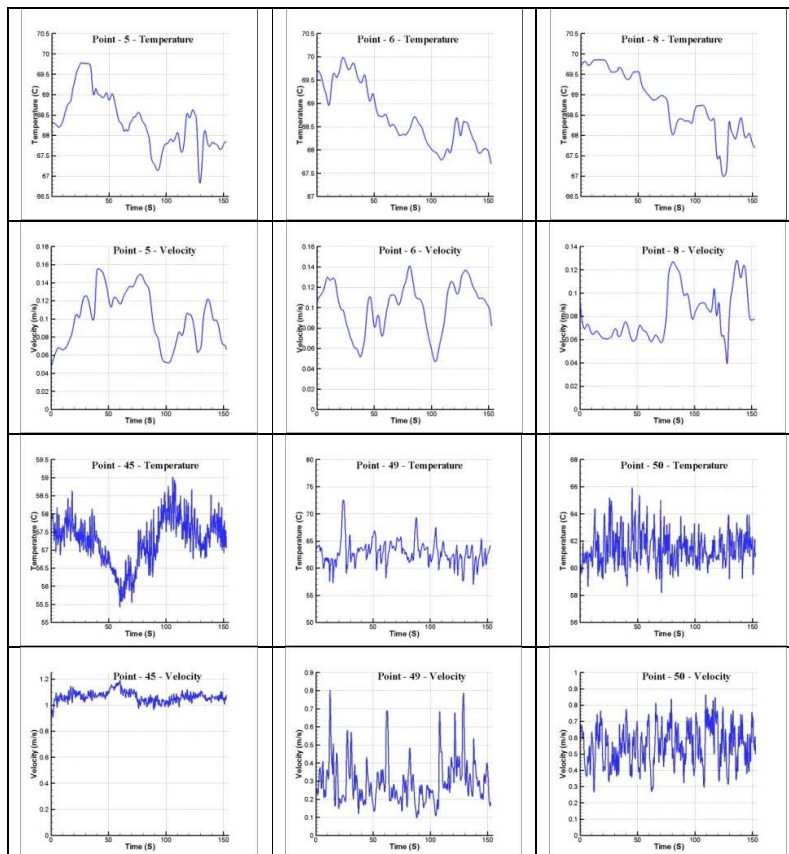


Fig. 4 Temperature and velocity fluctuations with time for various points

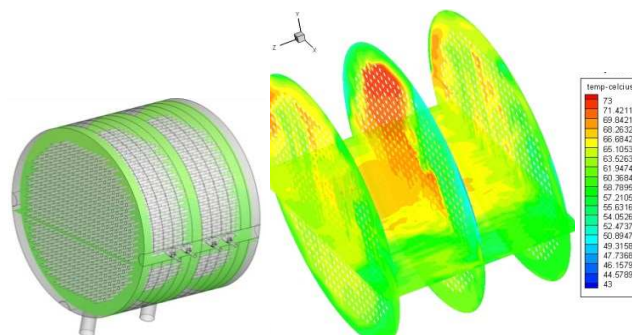


Fig. 5 Temperature distribution on 4 planes on Z and Y directions

ACKNOWLEDGMENT

The authors would like to thank Bruce Power Inc. and Candu Owners Group (COG) for their financial and scientific support of this project.

REFERENCES

- [1] D. Koroyannakis, R.D. Hepworth, and G. Hendrie, "An Experimental Study of Combined Natural and Forced Convection Flow in a Cylindrical Tank", AECL Report, TDVI-382, 1983.
- [2] C. Yoon, B. W. Rhee, H. T. Kim, J. H. Park, B. J. Min, "Moderator analysis of Wolsong units 2/3/4 for the 35% reactor inlet header break with a loss of emergency core cooling injection" *Journal of Nuclear Science and Technology* 43 (5), 505–513, 2006.
- [3] S. O. Yu, M. Kim, H. J. H. J. Kim, "Analysis of fluid flow and heat transfer inside Calandria vessel of CANDU-6 reactor using CFD", *Nuclear Engineering and Technology* 37 (6), 575–586, 2005.
- [4] H. F. Khartabil, W. W. Inch, J. Szymanski, D. Novog, V. Tavasoli, J. Mackinnon, "Three-dimensional moderator circulation experimental program for validation of CFD code MODTURC_CLAS. In: 21st CNS Nuclear Simulation Symposium", Ottawa, Canada, 2000.